

ORGANIC MASS SPECTROMETRY USING THE LASER MICROPROBE

David M. Hercules

Department of Chemistry, University of Pittsburgh, Pittsburgh, PA 15260, USA

Abstract - The use of a laser microprobe for analysis of organic microvolumes will be presented. The fundamental processes important to laser mass spectrometry of organic compounds and their "fragmentation processes" will be discussed. Examples of fragmentation will be considered in terms of the location of charge centers in organic molecules. A specific system to be addressed will be the amino acids. The relationship between SIMS and LMS spectra of amino acids will be treated. Results for quantitative analysis of organic materials using the laser microprobe will be presented. Included will be results correlated with HPLC studies and measurement of backwards versus forwards addition in polymer chains. Examples are presented to illustrate how the microprobe can obtain mass spectra from complex matrices. Included are results of mapping one organic compound on the surface of another. Use of solid-state reactions induced by the laser for chemical ionization of solids will be given. An example will be the use of nitrocompounds for obtaining useful negative ion spectra of polynuclear aromatic hydrocarbons.

INTRODUCTION

During the last fifteen years a prolific growth in ionization sources available for mass spectrometers has occurred. A major part of this growth represents development of "soft ionization" techniques which can be applied directly to solid state samples. A recent review has summarized development of these techniques through 1979 (1).

The first mass spectral technique that was widely applicable to nonvolatile substances was field desorption mass spectrometry (FDMS) (2). Although FDMS is applicable to a wide variety of materials, it presents serious operational problems to many laboratory. Thus, other solid state techniques were developed including plasma desorption mass spectrometry (PDMS) (3), secondary ion mass spectrometry (SIMS) (4), and the related technique, so-called fast atom bombardment (FAB) (5).

The use of a laser as an ionizing source in mass spectrometry is not new. Experiments were tried in the early 1960's (6) but suffered from experimental difficulties primarily due to the state of development of laser technology and time-of-flight mass spectrometers at that time. A recent review has summarized the historical development of laser mass spectrometry (7); recently development of commercial laser mass spectrometers has occurred (8,9).

Although all of these techniques have been available for at least a decade, there exists no clear understanding of the mechanisms involved in forming organic ions among the various techniques. Similarities among the spectra of the techniques suggest commonality of mechanism. Although the initial event in the energy transfer step must differ, conversion of this energy into excitons or phonons is probably responsible for the similarities among the techniques.

The present paper will stress the use of a commercial laser microprobe mass spectrometer (LAMMA^R-1000) for analysis of organic microvolumes. Important parameters must be considered when using a laser microprobe for organic mass spectrometry; the fragmentation processes involved, the relationship between LMS and other techniques, quantitation, how identifiable peaks from a component can be extracted from a complex matrix and ways to modify mass spectral behavior to render compounds identifiable by LMS. Also discussed will be the use of the organic microprobe to map the presence of an organic component on an organic surface.

LAMMA^R is a registered trademark of Leybold-Heraeus, GmbH

INSTRUMENTATION

The research reported here was obtained using a LAMMA-1000 (Laser Microprobe Mass Analyzer). This instrument uses a Q-switched laser as an ionization source, a microscope to focus radiation on the sample and a time-of-flight mass spectrometer to record spectra. It has the capability of providing both high spatial resolution and high sensitivity.

A schematic diagram of the LAMMA-1000 is shown in Figure 1. The instrument basically consists of four modules: the laser used for ionization, the sample and its associated optics, the time-of-flight mass spectrometer with its associated electronics and a detector-computer readout system. Each module will be discussed below.

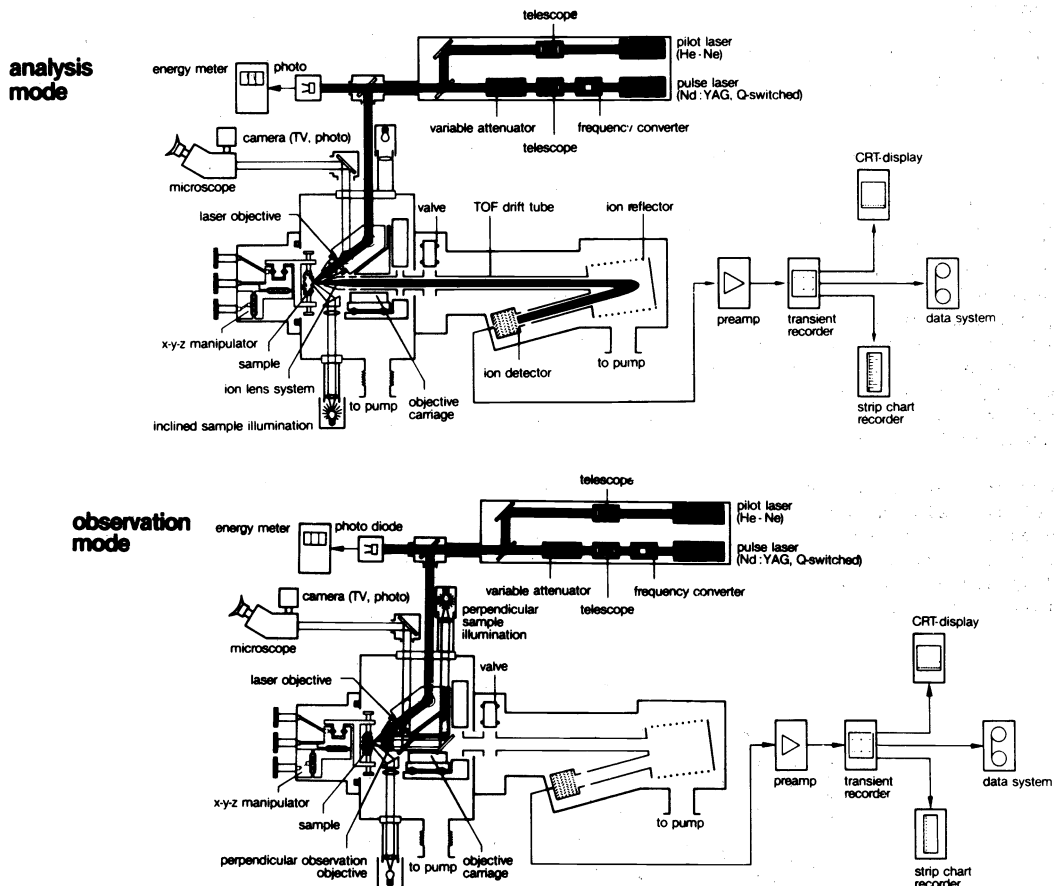


Figure 1. Diagram of the LAMMA-1000 laser mass spectrometry

A high-power (10^9 W/cm²) laser pulse (15 nanoseconds), provided by a frequency quadrupled ($\lambda = 265$ nm) Nd-YAG Q-switched laser, is focused on the sample. A pilot He-Ne laser follows the same optical path as the Nd-YAG laser to allow precise focusing of the laser pulse. A beam splitter provides a signal from the laser pulse to the photodiode which activates the time-of-flight mass spectrometer and records the pulse power on an energy meter. Reproducibility of the laser power is $\pm 8\%$ from shot to shot. Averaging multiple shots is important for quantitative analysis. A precise linear motion system is used to interchange the ion extraction system and the objective for sample observation. The instrument with the ion extraction system in place shown at the top of Figure 1 and sample observation mode is shown at the bottom. The microscope objective has an aperture of $f/0.22$ giving a resolution of about 2 microns on the sample. The intensity of the laser power can be varied continuously over three decades by a pair of twisted polarizers. The radiation is focused on the sample to an ellipse (approximately 2×3 μm axes) because of the 45° angle of the incident radiation.

A time-of-flight mass spectrometer is employed in the LAMMA-1000 to obtain a complete mass spectrum from a single laser shot. To achieve both high resolution and high transmission the analyzer uses an electrostatic focusing system for the ions. The ion reflector corrects for ions of the same mass which have different initial energies. Ion detection is accomplished by use of a Cu-Be secondary electron multiplier. The multiplier pulse is preamplified and stored in a transient recorder and ultimately read out by the computer. An HP series 1000 computer is used for data processing.

The LAMMA-1000 has a number of attractive features for chemical analysis. Virtually any type of sample can be run because the compartment can accommodate a sample up to 4 inches in diameter. Thus, one is not restricted to volatile or derivatized material or to materials which are optically transparent. At low laser powers (in the laser desorption mode) reproducible mass spectra can be obtained for organic and inorganic materials and their features can be related to molecular structure. An important feature is that both positive and negative ion spectra are obtained from the LAMMA-1000 having approximately equal intensities. Switching from positive to negative spectra is accomplished by push bottom selection.

By stepping the microscope stage in the x-y direction, it is possible to use the LAMMA-1000 as an organic microprobe. Of particular interest is the ability to obtain spectra from an organic material on an organic matrix. This type of problem is extremely difficult to do by other techniques, but as will be demonstrated here, can be accomplished with ease using the LAMMA-1000.

FUNDAMENTAL PROCESSES

Mechanism of laser ionization

The mechanism of laser ionization and volatilization of an organic solid is not well understood. A recent paper has summarized the current state of thinking about laser ionization processes (10). The conclusion is that much work still needs to be done on understanding mechanisms of laser ionization and how this can be applied fruitfully to improve understanding of ionization mechanisms. Some factors are known. For example, duration and shape of the laser pulse influence the type of spectra which are obtained. The process appears to be wavelength independent and the laser power density is probably the single most important parameter. Single photon absorption characteristics of the sample do not seem to correlate with LMS. The reason is that a variety of processes operate in laser ionization including volatilization, photoionization and shock wave effects.

There are several processes which occur simultaneously that give rise to the observed spectra. Using a very simplistic model one can consider that there are four important regions: 1) the region directly impacted by the laser, 2) secondary effects occurring in the region immediately adjacent to laser impact, 3) the surface of this adjacent region and 4) and a plume of material produced in the vacuum by laser volatilization. Figure 2 illustrates a conceptual model of these processes (11). Region 1 is the area of direct

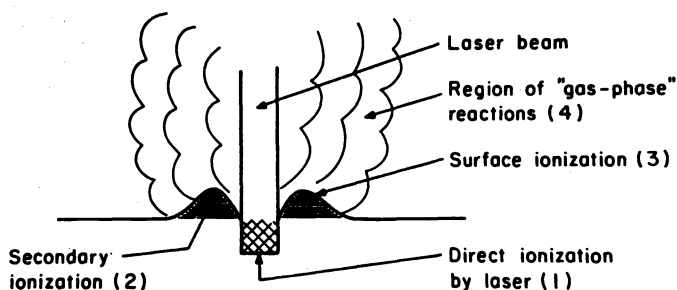


Figure 2. Model of laser ionization and volatilization (11)

interaction between the laser and the sample. Ionization undoubtedly occurs in this region and effective temperatures of approximately 7000°K have been proposed on the basis of an LTE model (12). This region will be characterized by extensive fragmentation and it seems likely that only atomic and small molecular fragments will be emitted from this region. At high power densities, the region of direct laser impact can truly be classified as a plasma.

Immediately adjacent to the region of direct laser interaction is an area of high thermal gradient. This region has been frequently referred to as the selvedge by some authors and can be looked upon as some sort of a condensed yet highly mobile phase. The selvedge is likely a fluid state of high temperature gradient where collisions can occur and which results in chemical reactions. This is probably where the majority of ions which are important to LMS are formed. The surface of this region (probably the true selvedge)

is a rapidly expanding region where the quasi-liquid sample becomes a "gas". It is difficult to distinguish between ionization reactions which occur directly at the surface and those occurring deeper in the sample.

Region 4 is the "cloud" produced by expulsion of material into the vacuum. It is clear that this is a region of rapid expansion going from a condensed phase (10^3 atm.) to 10^{-7} torr on the order of a few microns. This will be a region of rapid cooling. There is currently a debate over the significance of ion molecule reactions which occur in this "gas phase" region. Reactions must occur reasonably close to the surface where the gas density is fairly high.

Given the above model, it is reasonable that the time characteristics of particle emission will vary according to different regions. This is shown qualitatively in Figure 3. Ions

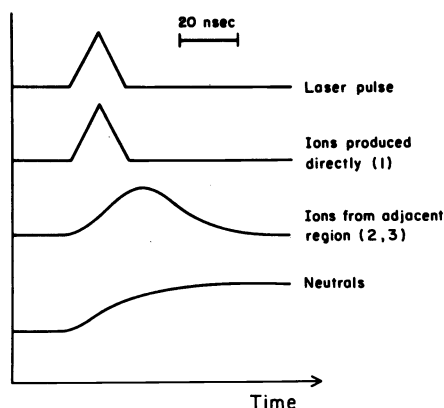
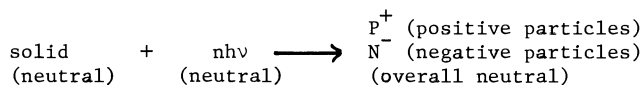


Figure 3. Time profiles of particle emissions in LMS (11)

produced in region 1 will be generated only while the laser is incident on the sample. Therefore, the time profile for emission of these ions should mimic the laser pulse exactly. Ion emission from regions 2 and 3 will also occur while the laser is incident on the sample. However, ion emission from this region should continue for a short time period after the laser pulse is extinguished and probably will not reach its peak at the peak of the laser pulse. Thus, one would expect to see a shift in time profile as shown in Figure 3. Emission of neutrals is a much lower energy process than ionization and neutral emission from the sample will continue as the thermal gradient established by the laser pulse dissipates through the sample. Thus, emission of neutrals will extend to much longer times as shown in Figure 3.

It is important to note that both negative ion and positive ion emission occur in LMS. Further, the threshold for generation of both types of ions is approximately the same and the relative intensities are also essentially the same. This effect arises because of the necessity for overall neutrality of the ionization process as illustrated in Table 1. A neutral solid is impacted by a photon (neutral) and charged particles are produced; equal numbers of positive and negative ions must result. Although photoionization could produce a large number of electrons, this is not the major ionization mechanism in LMS and thus one observes high yields of negative ions from organic molecules.

TABLE 1. Overall process in LMS



Ionization processes

Table 2 summarizes the major types of ionization processes observed in LMS. Ions are formed by one of the following processes: gain or loss of electrons, gain or loss of protons, direct ionization of salts, ion attachment reactions, or ion-molecule reactions.

Loss of electrons to form a molecular ion (similar to those observed in electron impact mass spectrometry) corresponds to photoionization; gain of electrons corresponds to electron attachment. A laser plasma has electrons of thermal energy (<1 eV) and attachment of thermal electrons to organic molecules is hypothetically possible. Thus, photoionization

TABLE 2. Ionization processes in LMS

<u>Gain or Loss of Electrons</u> $M \xrightarrow{nh\nu} M^+ + e^-$ $M + e^- \longrightarrow M^-$	<u>Gain or Loss of Protons</u> $MH + B \longrightarrow M^- + BH^+$ $M + BH \longrightarrow MH^+ + B^-$
<u>Ionization of Salts</u> $M^+X^- \xrightarrow{nh\nu} M^+ + X^-$	<u>Ion-Attachment Reactions</u> $M + C^+ \longrightarrow MC^+$ $M + A^- \longrightarrow MA^-$
<u>Ion-Molecule Reactions</u>	
$M \xrightarrow{nh\nu} A^+ + B^-$ $A^+ + M \longrightarrow AM^+$ $B^- + M \longrightarrow BM^-$	

should produce odd-electron positive molecular ions and electron attachment should produce odd-electron negative ions. However, simple gain or loss of electrons is not usually a major ion producing mechanism in laser mass spectrometry. In fact, it is usually the exception rather than the rule. Photoionization of aromatic hydrocarbons to produce odd-electron molecular ions is observed as can be seen from the spectrum of coronene in Figure 4. However, the corresponding electron attachment process is not usually observed for aromatic hydrocarbons and is quite rare for organic molecules in general.

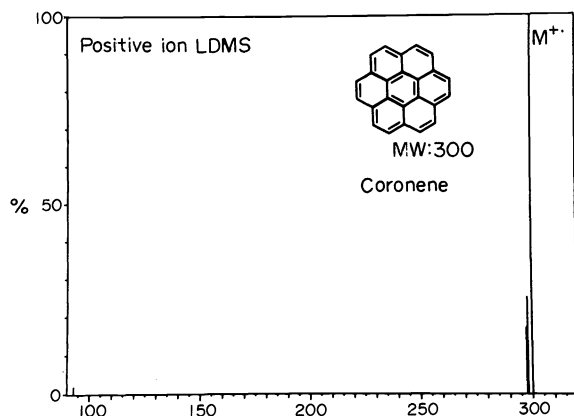


Figure 4. Positive-ion LMS of coronene

Probably the most important process for producing ions in LMS is gain or loss of protons. This is illustrated in Figure 5 for phenylalanine. Molecules having acidic functionalities ionize to produce negative ions and molecules having basic groups react with protons to produce positive ions. A key point of information is that ground state acid base behavior apparently is not the controlling process in laser ionization. Organic functional groups which are normally acidic or basic will so behave in laser ionization, but many groups show gain or loss of protons in LMS that is rarely seen in conventional chemistry. For example, benzylic hydrogens turn out to be quite acidic. In the example shown in Figure 5, it is clear that high yields of both $(M+H)^+$ and $(M-H)^+$ ions are observed for phenylalanine. This implies that protonation has occurred at the carboxyl group as has proton loss. Also, note that little else is seen in the negative ion spectrum except the $(M-H)^-$ ion and that fragmentation in the positive ion spectrum is small.

Another important mechanism is the ionization of organic salts. A salt consisting of a cation and an anion requires only that the laser provide energy to overcome the coulombic forces to produce the appropriate quasimolecular ion. Figure 6 shows the LMS of Safranin O; the peak at 314 corresponds to the molecular cation. Note also that in the case of Safranin O, little fragmentation has occurred. A fourth very important type of reaction in LMS is ion attachment. Here anions or cations can be attached to molecular species to produce a charged complex. Cation attachment reactions are more common in LMS,

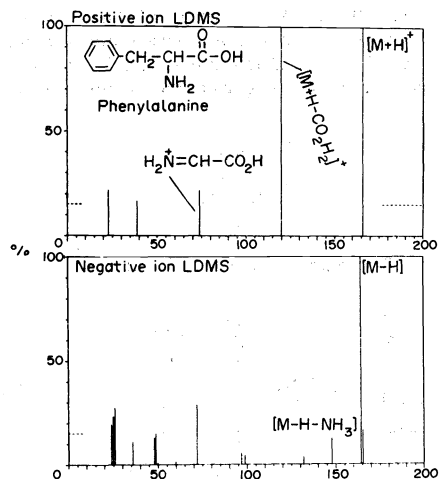


Figure 5. LMS of phenylalanine

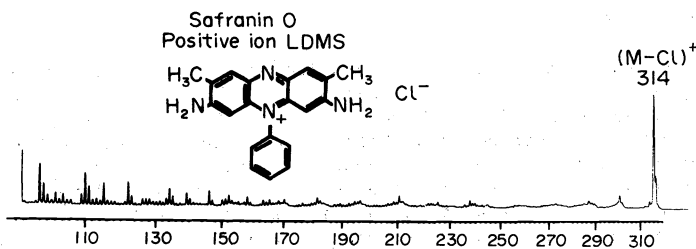


Figure 6. Positive LMS of safranin O

although anion reactions occur (13). Figure 7 shows the positive LMS of glycocholic acid showing sodium ion attachment. Note that cation attachment rivals the $(M+H)^+$ peak in intensity. Sodium ion attachment to hydroxyl containing compounds is quite common and can be used to obtain a laser mass spectra of high molecular weight glucocides.

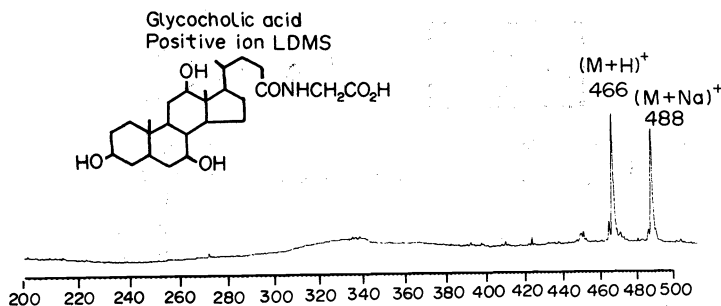


Figure 7. Positive LMS of glycocholic acid

Ion molecule reactions in LMS can either be beneficial or a nuisance. An ion molecule reaction occurs when a species A^\pm , is generated by the laser, in turn reacts with a species

of interest (M), forming a new ion MA^{\pm} . A spectrum of this type is illustrated in Figure 8 for a transition metal complex; the spectrum consists mainly of clusters of Co, I and CN. Although ion molecule reactions have not been used widely as an ionization process in LMS, the potential appears to be great for a number of reactions.

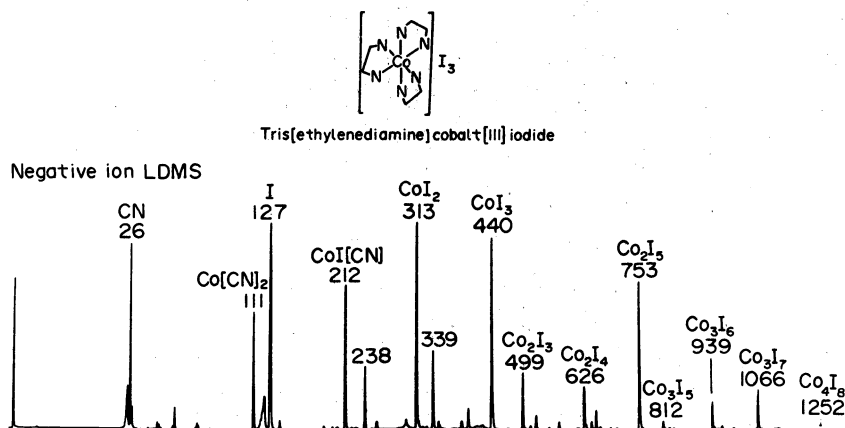


Figure 8. Negative LMS of tris(ethylenediamine)cobalt(III) iodide

FRAGMENTATION PROCESSES

This section will deal with some examples of "fragmentation" processes in laser mass spectrometry. The primary emphasis will be on the amino acids which represent one of the most extensively studied systems by LMS (14). When talking about fragmentation processes in LMS, one must remember that it is not certain whether one is dealing with a process which occurs for an isolated molecule in the "gas phase" over the surface or whether it is brought about in a condensed medium by a thermal process. Most likely it is a combination of the two. However, the net effect of fragmentation is similar to that observed in electron impact mass spectrometry and can be considered as though it were occurring for isolated molecules in the gas phase. There are clearly some "fragmentation processes" which must occur in a bi-molecular reaction. In this case it is quite probable that the reactions occur in the condensed phase and are similar to the ion molecule reactions discussed above.

The amino acids have been studied by several workers using laser mass spectrometry (15), although there has not been any detailed evaluation of fragmentation processes. We are in the process of completing a study of the fragmentation patterns of amino acids (14); we will deal here with simple aliphatic and aromatic amino acids.

Aliphatic amino acids show primarily three major peaks. The positive ion spectra show peaks corresponding to $(M+H)^+$ and $(M+H-HCOOH)^+$ and relatively few other fragment ions except m/z 30, $CH_2=NH_2^+$. Negative ion spectra show $(M-H)^-$ as the major feature and relatively minor fragmentation; loss of an aliphatic group is sometimes observed. A typical aliphatic amino acid fragmentation pattern is shown in Figure 9.

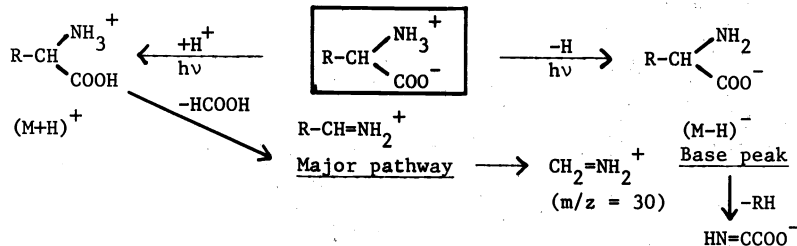


Figure 9. Fragmentation pattern for aliphatic amino acids

The simple aromatic amino acids show features comparable to those of aliphatic acids unless one has a large group such as tryptophane which then tends to dominate the spectrum. The nature of the aromatic group attached the amino acid can modify the fragmentation pattern significantly. An excellent example of this is shown in the LMS of phenylalanine and tyrosine. Fragmentation of phenylalanine is similar to the simple aliphatic amino acids

as shown in Figure 10. The only exception is that loss of ammonia and α,β -fission are much more pronounced. Figure 10 also shows the effect of a hydroxy group on the fragmentation of phenyl substituted amino acids, such as tyrosine. Note that substitution

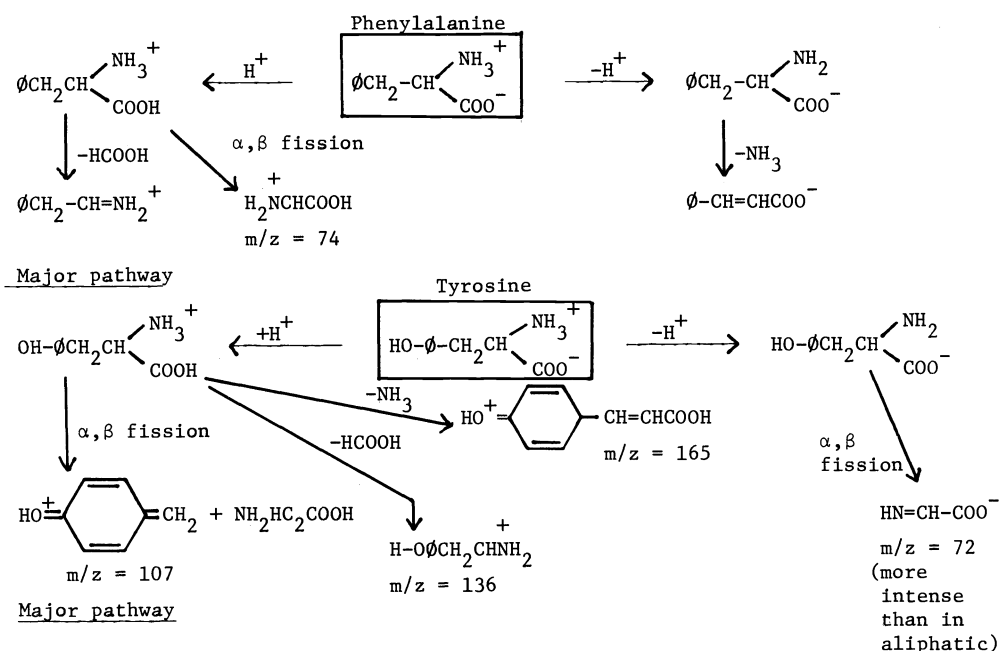


Figure 10. Fragmentation patterns of phenylalanine and tyrosine

affects the charge distribution in α,β -fission in the positive ion spectrum and introduces α,β -fission into the negative ion spectrum.

The major fragmentation mechanism of the α -amino acids can be viewed either as loss of formic acid from $(M+H)^+$ or loss of COOH from M^+ . Because peaks corresponding to M^+ are not observed in amino acid spectra, it seems reasonable that formic acid loss from the $(M+H)^+$ ion is the appropriate pathway. Given that formic acid loss is the major fragmentation mechanism, then the reaction should be influenced by the position of the amino group. This concept is based on the idea that the charge center on an ion will control fragmentation in LMS as it does in electron impact mass spectrometry. The effect of amino group position on fragmentation patterns for three amino acids is shown in Figure 11. The major fragment emission pattern clearly changes as the amino group is moved down the hydrocarbon chain. For example, in α -amino acids formic acid loss is

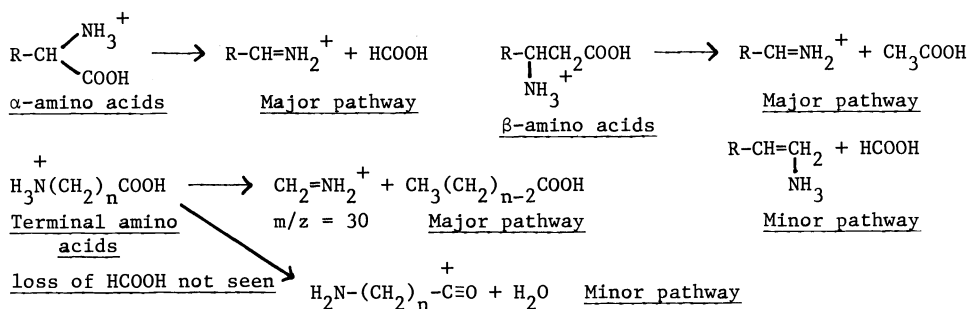


Figure 11. Effect of amino group position on fragmentation in LMS

major, for β -amino acids, acetic acid loss is major and for terminal amino acids loss of HCOOH is not seen, the fragment at m/z 30 is the base peak. Variation of major fragment elimination with the position of the amino group constitutes strong evidence that one is seeing fragmentation of the $(M+H)^+$ ion as opposed to fragmentation from M^+ . Reaction probably occurs through a 4-membered transition state which is common for even-electron ions. We have carried out deuteration studies which confirm that the proton transferred to the acid comes from the protonated group.

It is interesting to compare the LMS of amino acids with other mass spectral techniques (16). Table 3 presents a comparison between LMS, SIMS (17,18) and low energy electron impact mass spectrometry (LEEI) (19). It is interesting that there are similarities between LMS and SIMS, but significant differences between LMS and LEEI. Even at the low electron energies used in LEEI (2-4 eV) much greater fragmentation occurs than in the softer ionization techniques of LMS and SIMS.

TABLE 3. Comparison of LDMS, SIMS and LEEI

Positive Ions								
Aliphatic Amino Acids (Alanine)								
Technique	Major ions				Minor ions			
	M+H	M ⁺	M+H-CO ₂ H ₂	(M-H ₂ O) ⁺	M-R			
LDMS	100	0	92	0	0			
SIMS[7]	40	0	100	0	0			
LEEI[9]	100	17	0	52	81			
Aromatic Amino Acids (Phenylalanine)								
Technique					α - β fission	β - γ fission		
	M+H	M ⁺	M+H-CO ₂ H ₂	(M-H ₂ O) ⁺				
LDMS	100	0	100	0	21 α	0		
SIMS[7]	30	0	100	0	56 β	37		
(Benninghoven)								
SIMS[8]	84	0	100	4	27 β	20		
(Klöpffel)								
LEEI[9]	64	37	94	16	93(α)	100(β)	ND	
Negative Ions								
Aliphatic Amino Acids (Alanine)								
Technique	M-H	M ⁻	M-R-R		M-R	M-NH ₂	M-CO ₂ H	R ⁻
			(m/z 72)	M-H ₂ O				
LDMS	100	0	0	0	0	0	0	0
SIMS[7]	100	0	0	0	0	0	0	0
LEEI[9]	100	18	0	2	16	49	0	0
Aromatic Amino Acids (Phenylalanine)								
LDMS	100	0	29	0	0	0	0	0
SIMS[7]	100	0	0	0	0	0	0	0
LEEI[9]	100	20	0	0	29	6	3	12

A significant point is the high intensity of M⁺ ions in LEEI in the positive ion spectra of both aliphatic and aromatic acids but not in the LMS or SIMS spectra. Although the major loss from (M+H)⁺ in SIMS and LMS is formic acid, in LEEI it is loss of water and the alkyl sidechain R. LEEI shows significant formic acid loss in phenylalanine, but also shows much more loss of water than either SIMS or LMS. Another significant difference is that in LEEI only α , β -fission is observed for phenylalanine, whereas in SIMS both α , β - and β , γ -fission are observed. In LMS, only α , β -fission is observed similarly to LEEI.

In the negative ion spectra, M⁻ is observed in LEEI for both aliphatic and aromatic acids. Neither SIMS nor LMS shows any other fragmentation process; (M-H)⁻ is the major peak. LEEI, however, shows significant loss of the aliphatic chain group R, loss of NH₂ and in the case of phenylalanine the presence of R⁻.

On the basis of the data presented in Table 3, one can conclude that the ionization processes responsible for LEEI are different from those of LMS and SIMS and that the latter are probably similar. Another important point that the data make is that SIMS and LMS represent much softer ionization techniques than even low energy electron impact mass spectrometry.

QUANTITATIVE ANALYSIS

Laser mass spectrometry has the potential for performing rapid quantitative analyses on nonvolatile or thermally labile materials. Although LMS is ideally suited to semi-quantitative analysis of trace metals in a variety of matrices (20), very little work has been reported for quantitative analysis of organic compounds. Recently we have reported quantitative analysis of a mixture of two quaternary ammonium salts (λ and ν) and have compared the results for this mixture with high performance liquid chromatography (HPLC) (21).



Figure 12 shows the HPLC separation of the mixture of the benzylammonium chlorides. UV absorption of the benzyl moiety was used for detection and thus the integrated areas under the peaks correspond to relative amounts of material. HPLC yielded a ratio of $\mathbf{2}:\mathbf{1}$ of 3.0.

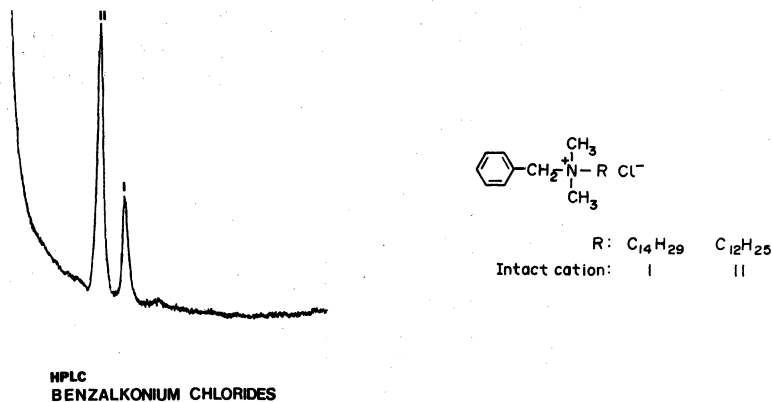


Figure 12. HPLC separation of the benzylammonium chlorides $\mathbf{1}$ and $\mathbf{2}$ (21)

It was of interest to determine whether or not C_{10} and C_{16} derivatives similar to $\mathbf{1}$ and $\mathbf{2}$ could be detected by HPLC; the sample was indicated to be a two component mixture. A possible small contamination of the C_{16} component can be seen in the small peak immediately to the right of compound $\mathbf{1}$. However, this is barely above noise.

Figure 13 shows the positive LMS of the benzylammonium chloride mixture. This was obtained by averaging 12 spectra. The cations of the two compounds appear at m/z 304 ($\mathbf{2}$) and m/z 332 ($\mathbf{1}$). Loss of toluene occurs in both cations giving peaks at m/z 240 and 212 for $\mathbf{1}$ and $\mathbf{2}$, respectively. The base peak at m/z 91 is the familiar benzyl (tropylium) moiety as would be expected on the basis of electron impact mass spectrometry.

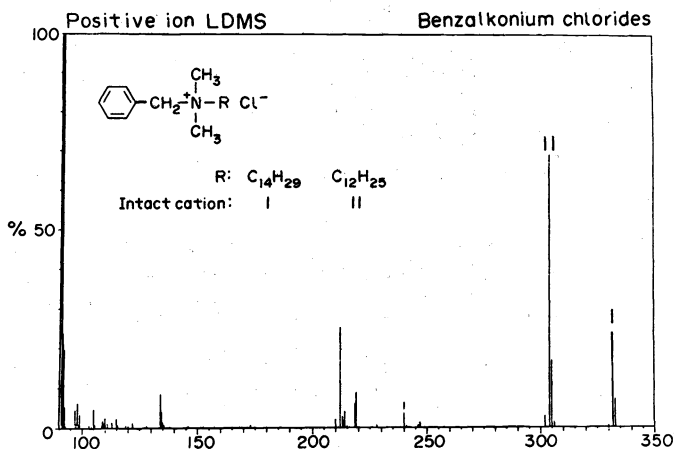


Figure 13. Positive LMS of the benzylammonium chloride mixtures (21).

The intensity ratio of the two cation peaks has been used to calculate the relative ratio of the two components in the mixture; the ratio measured by LMS is $\mathbf{2}:\mathbf{1} = 2.9 \pm 0.3$. It is clear that this is within experimental error of the value derived from HPLC and demonstrates that LMS can be applied to quantitative analysis of mixtures of organic compounds.

An important problem in polymer science is probing the molecular chain structure of polymers. Polyvinylidene fluoride (PVF₂) is produced by a free radical polymerization process yielding a linear polymer consisting of repeating CH₂CF₂ monomer units. The preferred polymer chain orientation is head-to-tail, i.e. -CH₂CF₂CH₂CF₂- with the CF₂ group being referred to as the head and the CH₂ group as the tail. All PVF₂ chains contain a small percentage of backward additions, namely, head-to-head and tail-to-tail, which can affect polymer properties. Quantitative measurement of the PVF₂ molecular chain structure has been accomplished through ¹⁹F NMR (22). NMR results showed that backward additions constitute about 4-6% of the chain and that these backward units are well separated along the chain. We were interested in seeing if LMS could perform quantitative analysis of the backward addition units in the PVF₂ chain. Such a mass spectrometric method would represent a simple, quick method involving minimal sample preparation.

Four commercial PVF₂ samples were used to compare LMS with ¹⁹F NMR. The samples ranged in percentage of backward addition from 2.5-4.8%. The LMS spectra were obtained using the LAMMA-1000; a typical PVF₂ spectrum is shown in Figure 14. The major feature in the

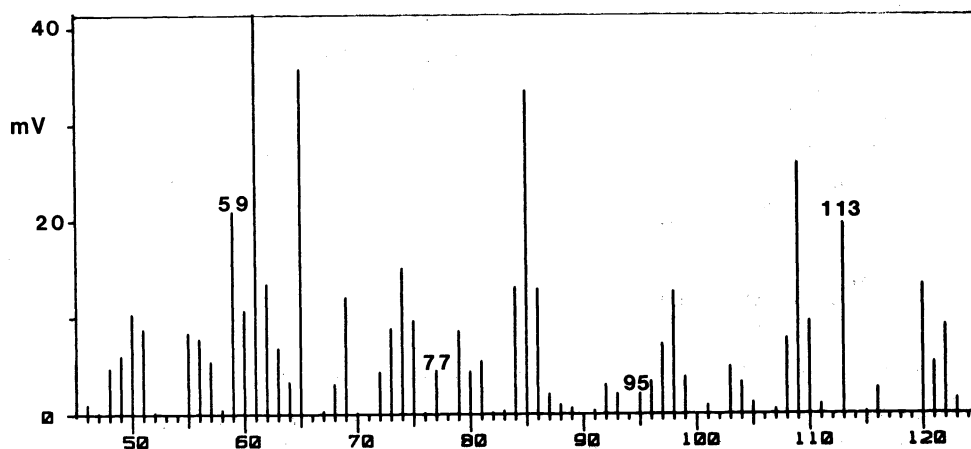


Figure 14. Positive LMS of poly(vinylidene fluoride).

PVF₂ spectrum (as with other fluoropolymers) is the presence of three carbon fragments which are indicative of the polymer molecular structure. In the case of PVF₂ each fragment has a unique mass allowing for quantitative measurement of their ratio. The important positive ion fragments pertaining to the structure of PVF₂ are: CF₂CHCF₂⁺ (m/z = 113), CF₂CFCH₂⁺ (m/z = 95), CF₂CHCH₂⁺ (m/z = 77) and CH₂CFCH₂⁺ (m/z = 59). The m/z = 113 and 59 ions arise from normal linkages while the m/z = 95 and 77 ions correspond to head-to-head and tail-to-tail linkages, respectively.

The ideal equation for determining the percentage of backwards addition via mass spectrometry would be:

$$\%B = \frac{\sum_{\text{HHTT}} (I)}{\sum_{\text{HHTT}} (I) + \sum_{\text{HT}} (I)} = \text{percent backwards addition} \quad (1)$$

where I = the ion intensity in counts, and HT and HHTT correspond to ions from normal and backwards additions, respectively. Unfortunately, fragment ions are not produced either as fragments or as ions with equal efficiency, so it is necessary to add two terms to correct for these factors. Therefore, the operational equation is:

$$\%B = \frac{\sum_{\text{HHTT}} \left(\frac{I}{C^2}\right)^\alpha}{\sum_{\text{HHTT}} \left(\frac{I}{C^2}\right)^\alpha + \sum_{\text{HT}} (I)^\alpha} \quad (2)$$

The α term was calculated to be 1.04 and C term corresponds to the number of carbon atoms in the ion, three in this case. These values were obtained from a known sample of PVF₂ having a known percentage of backwards and forward addition. Data obtained on four samples are presented in Table 4:

TABLE 4. Comparison of NMR and LAMMA Analysis for Polyvinidene Fluoride

	Polymer Sample				r.s.d
	A	B*	C	D	
%B LAMMA Analysis	2.4	4.0	4.3	4.8	+0.1
%B ¹⁹ F NMR	2.5	4.0	4.7	4.8	+0.02

* This polymer sample was used as a standard

The LAMMA and NMR results for samples A and D agree quite well. Sample C shows deviation of 0.4% which is outside the statistical limits anticipated on the basis of the other samples. It is possible that sample C may have a higher degree of branching incorporated into the structure, thus deviating from the necessary assumption of a linear polymer. Nevertheless, the close agreement between the two methods demonstrates the capability of LMS for doing quantitative analysis of units in a polymer chain if the appropriate mathematical model can be constructed and the proper standards are available.

SOLID STATE CHEMICAL IONIZATION SOURCES

Laser mass spectra of organic compounds containing electron withdrawing groups frequently yield odd electron molecular anions ($M^{\cdot-}$) in conventional negative EI mass spectrometry. A class of compounds typical of this behavior is the nitrobenzene derivatives. Because of this we elected to study the negative ion LMS of a series dinitrobenzenes and related compounds. Surprisingly, neither the molecular anion nor the quasimolecular anion was observed. Common peaks in the negative ion LMS of the substituted nitrobenzenes were CN^- ($m/z = 26$), OCN^- ($m/z = 42$), NO_2^- ($m/z = 46$), C_3N^- ($m/z = 50$) and $(M-NO)^-$ where $M =$ molecular weight). An additional intense peak was observed at $(M+15)^-$ initially for o-dinitrobenzene, 1,8-dinitronaphthalene, and 1,3,5-trinitrobenzene. The negative ion LMS of o-dinitrobenzene is shown in Figure 15 as an example. The peak at $m/z = 183$ corresponds to $(M+15)^-$.

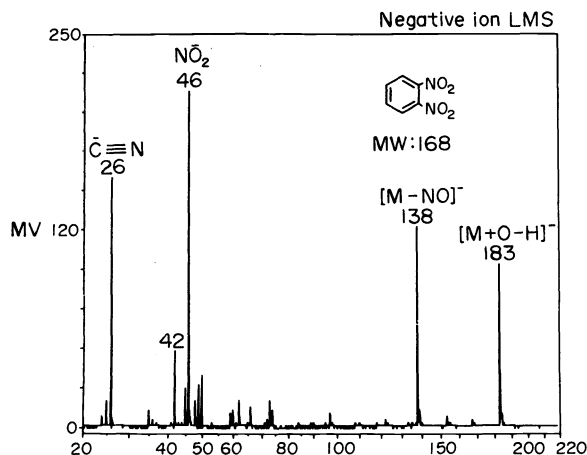


Figure 15. Negative LMS of o-dinitrobenzene

Formation of $(M+15)^-$ can be interpreted as substitution of an oxygen atom onto the aromatic ring initiated by the laser. The formal representation of the peak would be $(M+O-H)^-$. The reaction can be viewed as a nucleophilic substitution reaction occurring in the solid region of the sample impacted by the laser, or less likely as a gas phase reaction. Formation of $(M+15)^-$ is possible by one of three mechanisms; at present it is not possible to distinguish between them:



In contrast, the negative ion LMS of m- and p-dinitrobenzenes do not show a significant peak corresponding to $(M+15)^-$. Thus, it is clear that some interaction of nitro groups is important. A series of dinitro aromatics was studied to further elucidate the effect of structure. Figure 16 summarizes the results of these studies. Those compounds in the boxes show the presence of $(M+15)^-$ whereas those without the boxes do not. It is clear

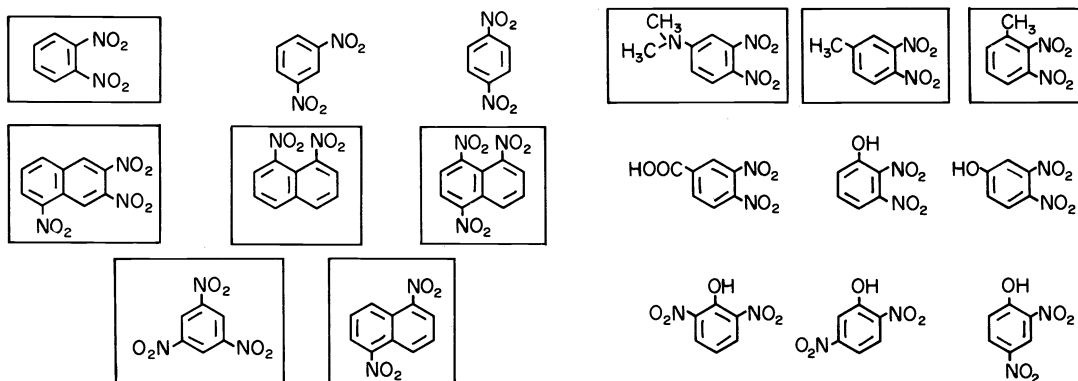


Figure 16. Nitroaromatic structures studied by LMS. Those compounds enclosed in boxes show significant peaks corresponding to $(M+O-H)^-$.

that formation of $(M+15)^-$ is facilitated by two nitro groups adjacent to each other (either ortho or peri) but this is not mandatory. It is also clear that when competing proton abstraction reactions are possible an $(M+15)^-$ peak is absent. This can be seen in the case of compounds containing phenolic or carboxylic hydrogens. This is obviously an interesting effect of laser induced chemistry, but considerable more work is necessary to elucidate the exact mechanism(s) of the reaction.

Polynuclear aromatic hydrocarbons generally do not show negative molecular ions in LMS even though the negative ions of these compounds are stable in solution. Virtually all polynuclear aromatic hydrocarbons having three or more rings have positive electron affinities and thus one would expect stable molecular ions in the gas phase. However, a series of carbon cluster ions corresponding to C_n^- and C_nH^- constitutes the negative ion spectra of polynuclear aromatic hydrocarbons. Although molecular ions (M^-) can be observed in LMS, the peaks are usually weak and their appearance is rare.

The formation of charge transfer complexes between aromatic hydrocarbons and electron donors (N,N,N,N-tetramethyl-p-phenylenediamine) (TMPD) and 1,3,5-trinitrobenzene (TNB) respectively is well known. In an attempt to induce charge transfer reactions in LMS, a series of polyaromatic hydrocarbons was obtained mixed with TMPD and TNB. The presence of TMPD had essentially no effect for aromatic compounds with the exception of those containing benzylic hydrogens which showed $(M-H)^-$ peaks. Addition of TNB caused the presence of a peak at $(M+15)^-$ (where M corresponds to the aromatic hydrocarbon) as was observed for many of the nitro substituted compounds. An example of this is shown in Figure 17 for coronene mixed with TNB. The peak at m/z 315 corresponds to $(M+15)^-$ and the base peak at $m/z = 183$ corresponds to $(M-NO)$ from TNB.

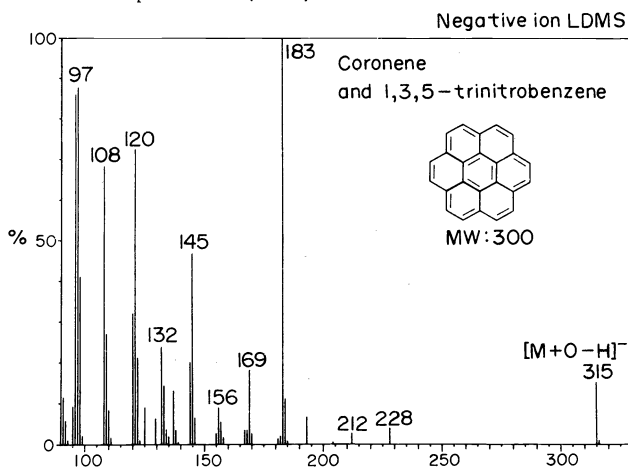


Figure 17. Negative LMS of coronene mixed with 1,3,5-trinitrobenzene.

We have studied upwards of 20 polynuclear aromatic hydrocarbons and have observed oxygen transfer when mixed with 1,3,5-trinitrobenzene. We also attempted to use other species in this reaction such as Na_2O , $NaNO_3$, $NaNO_2$ and a nitrocellulose polymer. All of the

above gave the same result, namely, formation of a peak corresponding to $(M+O-H)^-$. The negative ion LMS of the reagents show formation of three potential reactants: $O^{\cdot-}$, $O_2^{\cdot-}$ and NO_2^- . Thus, the same three potential substitution mechanisms as stated above (reactions 3-5) could be operative. However, no correlation between the relative amounts of these species and the $(M+O-H)^-$ peak was found in the compounds studied. Thus, it is difficult to say whether the reaction is an analog of solution chemistry induced thermally, or if it is brought about by species in the excited state. Nevertheless, this represents the possibility of the chemical ionization reaction induced by the laser which can be used as an ionizing source for mass spectrometry. Preliminary studies, in our laboratory, for other sources have indicated that this type of reaction is quite general and opens up the possibility for using chemical ionization in solid state mass spectrometry.

DIRECT LMS ANALYSIS OF SOLID MATERIALS

A distinct advantage of the LAMMA-1000 and its front surface configuration is the ability to perform direct analysis of solids. Essentially, any sample that can be inserted into the sample chamber, brought under a vacuum and placed into the focus of the laser, can be analyzed by laser mass spectrometry. This capability opens numerous possible uses for the laser microprobe which have not been accessible by more conventional mass spectral techniques. We are currently involved in three such areas: coupling of LMS with thin layer chromatography, direct LMS analysis of naturally occurring materials, and development of an organic microprobe. Examples of how it is possible to perform these types of analysis will be presented below.

Combinations of separation techniques and mass spectrometry have proved valuable for analytical chemistry. Numerous couplings of separation techniques and mass spectrometer have demonstrated the power and utility of this approach (23-27). Several recent reviews (23-25) have discussed the various approaches to coupling GC and LC with mass spectrometers. Several authors have recently dealt with the problem with coupling LC directly with LMS (28,29). A very promising combination is the direct coupling of thin layer chromatography (TLC) with the laser microprobe.

TLC is probably the most widely used separation method because of its utility and the ease of experimental operation. Its flexibility exceeds either LC or GC and making it the most powerful separations method available to the practicing chemist. Thus, it would be extremely valuable to couple this powerful and widely used separation technique directly to a mass spectrometer. It is possible to couple TLC and LMS indirectly and the utility of this combination has already been shown (27). However, no examples of the direct combination of TLC and LMS have been reported.

TLC has been a traditional source of frustration to analytical chemists. Frequently, small spots are observed which do not correspond to components detected by LC or GC, identification is difficult and quantitation almost impossible. Considerable effort has been expended scraping spots from TLC plates, extracting and attempting to identify or measure the material by a combination of conventional spectroscopic techniques. Thus, direct analysis of TLC plates by LMS is particularly intriguing.

The combination of high performance thin layer chromatography (HPTLC) with the LAMMA-1000 should provide a means of increasing chromatographic resolution due to the inherent lateral resolution of the LAMMA microprobe. Indeed, the combination of HPTLC and LMS represents a separations-spectroscopic combination which has potential exceeding either GC/MS or LC/MS. We present here initial results on the direct analysis of samples from an HPTLC plate.

Organic dyes represent an ideal case for studying the combination of HPTLC and LMS. The presence of ionic groups normally limits the use of conventional mass spectrometry for dyes but make them ideal for analysis by LMS. Because dyes are colored, it is easy for one to detect spots on HPTLC plates. One class of dyes having readily obtained LMS spectra are the triphenylmethane dyes (30). The standard method for separating and identifying this class of dyes is TLC (31). Thus, one can use this system to confirm an assignment based on R_f by obtaining a mass spectrum of the spot.

A mixture of seven dyes was used: methyl violet, brilliant green, ethyl violet, gentian violet, rosaniline hydrochloride, malachite green, and victoria blue B. These dyes have been characterized by LMS (30) and are separated on an HP-K Whatman HPTLC plate according to a well-defined method (31). The air dried HPTLC plate was subsequently analyzed by LMS. Table 5 lists the dyes studied and their quasimolecular ion peaks. Figure 18 shows the positive ion TLC LMS spectra of two dyes; the quasimolecular ions are well defined and relatively few fragment ion peaks are observed.

TABLE 5. Quasimolecular Ions (M^+) for Triphenylmethane Dyes

Dye	M^+ (m/z)
Rosaniline Hydrochloride (RH)	302
Malachite Green (MG)	329
Brilliant Green (BG)	345
Methyl Violet (MV)	358
Gentian Violet (GV)	372
Ethyl Violet (EV)	456
Victoria Blue B (VB)	470

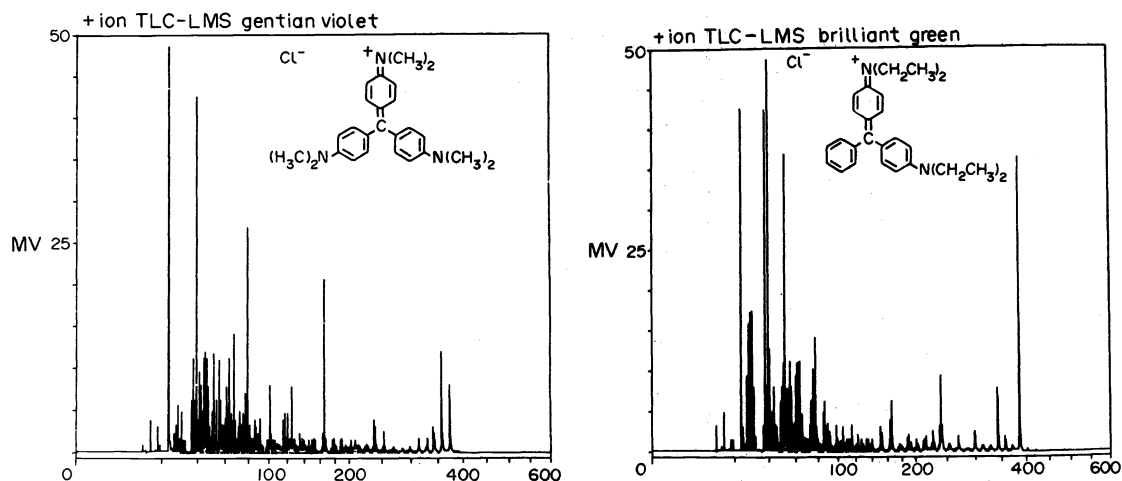


Figure 18. Positive ion TLC-LMS spectra of gentian violet and brilliant green

Figure 19 shows a diagram of a typical HPTLC plate containing a mixture of the seven dyes. The spots corresponding to the various dyes are listed on the left hand side of the figure. On the right hand side of the figure are the peaks observed in the LMS spectra obtained at various locations along the HPTLC plate. Peaks are listed for the range m/z 300 to 600 which corresponds to the quasimolecular ions of the dyes. As is seen from Figure 19, spectra taken in the regions between spots showed no LMS peaks in this region except where spots overlap. There, quasimolecular ions of both dyes are observed. Thus, it is clear that LMS detects the presence of the dyes and that background interference from the HPTLC plate is negligible.

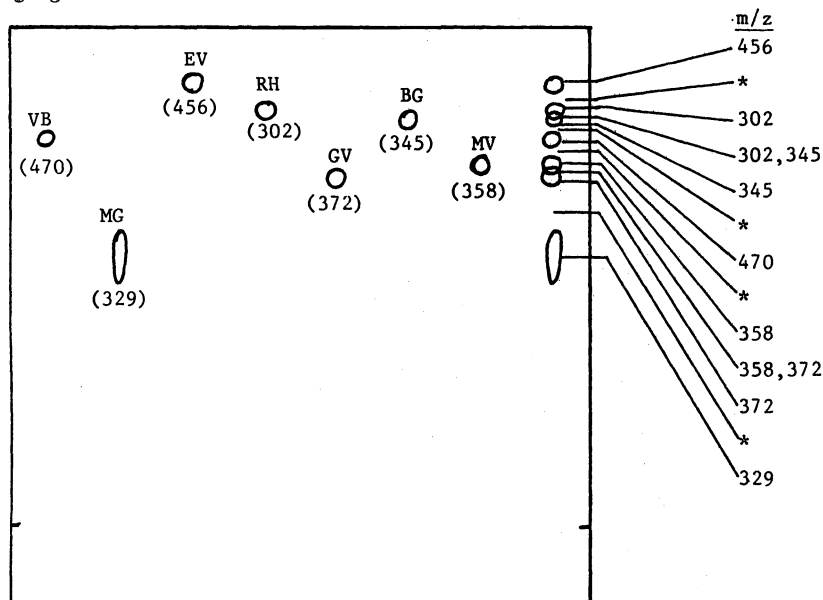


Figure 19. HPTLC/LMS analysis of dye mixtures

These initial results clearly demonstrate the possibility of employing LMS as a detector for HPTLC. Further work is underway in our laboratory to define the nature of samples for which the technique can be used and to determine detection limits for the HPTLC/LMS combination.

The encouraging results on direct analysis from TLC plates prompted investigation of other possibilities for the direct application of LMS to solid matrices. One possibility considered was the direct analysis of plant materials to identify and/or determine specific chemicals present in these plants. Because of the microprobe capabilities of the LAMMA-1000, it should be possible to do this type of analysis on microscopic plants. The example illustrated here will be for the detection of caffeine directly from a coffee bean.

Figure 20 shows the negative LMS of a coffee bean. The mass spectrum clearly corresponds to the negative ion LMS of caffeine as indicated by the peaks in the figure. This example represents only qualitative detection of caffeine and does not deal with the problem with quantitative analysis in such a matrix. This type of analysis will be possible only if

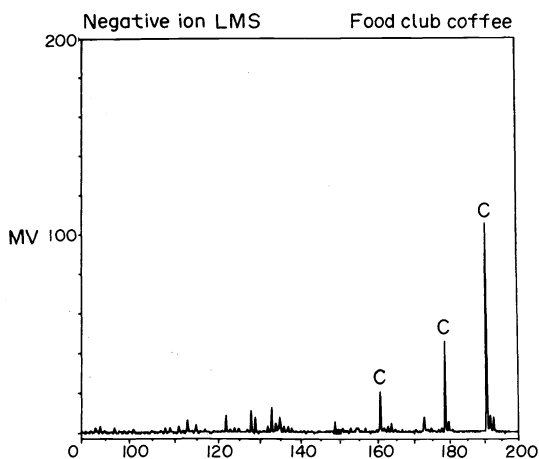


Figure 20. Negative ion LMS spectra of brand name coffee bean

internal standard techniques for such materials can be developed. However, it represents one of a variety of samples from which spectra can be obtained directly. It opens up intriguing possibilities for direct analysis of herbicides and pesticides from plants, microscopic examination of these materials in plant tissue, and analysis of portions of microscopic plants for specific organic materials.

The LAMMA-1000 has demonstrated its ability to image a variety of solid samples including organics. For example, it has been possible to correlate presence of an organic component in inflamed tissue and its lower level in normal tissue (32). This raises the possibility of using the LAMMA-1000 to map one organic material in a matrix of another. This can be accomplished on the microscale because of the high spatial resolution of the instrument. Thus, the use of the laser ionization source as a mapping technique should make available to investigators concerned with organic contaminants the type of information available from Auger or SEM/EDX combination for elemental analyses.

To demonstrate the microprobe mapping capabilities of LMS, a polystyrene film was cast from solution and organic dyes were deposited on the film at various locations. Deposition and accurate placement of the dyes was performed using a microsyringe combined with a micromanipulator. The diameter of the microsyringe tip is approximately 20 μm which permitted us to readily deposit spots of approximately 50 μm diameter. Several spots were deposited in a small area approximately 1 mm square and this region on the polystyrene film was mapped using LMS. A complete mass spectrum was collected at every point and points were incremented by 25 μm .

The results of LMS mapping showed the typical mass spectral pattern for polystyrene at every point. This consists of the characteristic carbon clusters as well as the uniquely defined peaks at 77 and 91 corresponding to the phenyl and benzyl peaks. These peaks are characteristic of polystyrene (33). In general, at the power levels used, polystyrene showed peaks only below m/z 150.

In addition to the polystyrene peaks, those areas that had been spotted with the dye also revealed a molecular ion corresponding to the dye, as well as fragments typical of the particular dye. The peaks characteristic of the dyes were in the m/z 300-600 region and thus were not interfered with by the polymer fragments. Qualitatively, this shows that

it is possible to obtain characteristic peaks of a material in a mapping experiment and that combinations of peaks can be used to identify a particular species. For example, for gentian violet, two typical peaks are seen at m/z 372 and m/z 356 occurring in the ratio of 2:1. In a mapping experiment on polystyrene, identical peaks and peak ratios were observed. Thus, the combination of peaks could be used to map this dye on a polymer matrix.

Displaying the area map graphically illustrates where the dyes are located on the polymer. It also allows one to differentiate easily among the different organic dyes by their quasimolecular and fragmentation patterns. When spots from two dyes overlap, they could be identified by peaks corresponding to both dyes.

The three examples illustrated here clearly indicate the potential for application of LMS to a variety of analytical problems. Because the LAMMA-1000 can obtain spectra directly from solids, it represents a potentially valuable tool for characterization of a wide variety of solid-state materials.

Acknowledgement - I would like to acknowledge the assistance of the following people in obtaining the data used in this presentation: K. Viswanadham, F. Novak, K. Balasanmugam, D. Mattern, B. Wilk, and F. Lin. I also wish to acknowledge with appreciation support of this research by the National Science Foundation and the Office of Naval Research.

REFERENCES

1. G. D. Daves, Jr., Accts. Chem. Res. **12**, 359-65 (1979).
2. H. D. Beckey, Int. J. Mass Spectrom. Ion Phys. **2**, 500-503 (1969).
3. R. D. Mcfarlane, C. J. McNeal, J. E. Hunt, Adv. Mass Spectrom. **8A**, 349-54 (1980).
4. A. Benninghoven, D. Jaspers, W. Sichtermann, Appl. Phys. **11**, 35-39 (1976).
5. M. Barber, R. S. Bordoli, R. D. Sedgwick, A. N. Tyler, J. Chem. Soc. Chem. Comm. 325-27 (1981).
6. R. E. Honig, J. R. Woolston, Appl. Phys. Letters **2**, 138 (1963).
7. R. J. Conzemius, J. M. Capellen, Int. J. Mass Spectrom. Ion Phys. **34**, 197-271 (1980).
8. H. Vogt, J. H. Heinen, S. Meier, R. Wechsung, Z. Anal. Chem. **308**, 195-200 (1981).
9. H. J. Heinen, S. Meier, H. Vogt, R. Wechsung, Proc. 9th Intl. Mass Spectrom. Conf., Vienna, Austria (1982).
10. F. Hillenkamp, Int. J. Mass Spectrom. Ion Phys. **45**, 305-313 (1982).
11. D. M. Hercules, R. J. Day, K. Balasanmugam, T. A. Dang, C. P. Li, Anal. Chem. **54**, 280A-288A (1982).
12. J. F. Ready, Effects of High-Power Laser Radiation, Academic Press, New York (1971).
13. K. Balasanmugam, T. A. Dang, R. J. Day, D. M. Hercules, Anal. Chem. **53**, 2296-2298 (1981).
14. C. D. Parker, D. M. Hercules, to be published.
15. C. Schiller, K. G. Krupke, F. Hillenkamp, Z. Anal. Chem. **308**, 304 (1982).
16. D. M. Hercules, C. D. Parker, K. Balasanmugam, S. K. Viswanadhan, in A. Benninghoven, ed., Ion Formation from Organic Solids, Springer-Verlag, Berlin, pp. 222-228 (1983).
17. A. Benninghoven, D. Jaspers, W. Sichtermann, Appl. Phys. **11**, 35 (1976).
18. D. K. Klöppel, G. Von Bülow, Int. J. of Mass Spect. and Ion Phys. **39**, 85 (1981).
19. D. Voigt, J. Schmidt, Biomed. Mass Spectrom. **5**, 44 (1978).
20. R. Kaufmann, F. Hillenkamp, R. Wechsung, Med. Prog. Technol. **6**, 109-21 (1979).
21. K. Balasanmugam, D. M. Hercules, Anal. Chem. **55**, 145-146 (1983).
22. C. W. Witson, J. Polymer Sci. A **1**, 3105-1310 (1963).
23. M. C. Ten Noever de Brauw, J. Chromatogr., Chromatogr. Rev. **165**, 207-233 (1979).
24. N. M. M. Nibbering, J. Chromatogr., Chromatogr. Rev. **251**, 93-104 (1982).
25. H.-R. Schulten, J. Chromatogr., Chromatogr. Rev. **251**, 105-128 (1982).
26. P. J. Arpino, G. Guiochon, Anal. Chem., **51**(7), 682A-701A (1979).
27. D. A. Durden, A. V. Juovio, B. A. Davis, Anal. Chem. **52**, 1815-1820 (1980).
28. J. F. K. Huber, T. Dzido, F. Hevesch, J. Chromatogr. **271**(1), 27-33 (1983).
29. E. D. Hardin, Laser Desorption Mass Spectrometry of Nonvolatile Biomolecules, Dissertation, University of Houston, (1981).
30. F. P. Novak, D. M. Hercules, unpublished results.
31. H. Schweppe, Thin-Layer Chromatography, in K. Venkatvaman, ed., The Analytical Chemistry of Synthetic Dyes, John Wiley & Sons, New York, pp. 23-56 (1977).
32. U. Seydel, B. Lindner, in A. Benninghoven, ed., Ion Formation from Organic Solids, Springer-Verlag, Berlin, pp. 240-244 (1983).
33. J. A. Gardella, D. M. Hercules, Z. Anal. Chem. **308**, 297 (1981).